High-Temperature-Stable Au@SnO2 Core/Shell Supported Catalyst for CO Oxidation

ARTICLE *in* THE JOURNAL OF PHYSICAL CHEMISTRY C · JANUARY 2008

Impact Factor: 4.77 · DOI: 10.1021/jp711880e

5 AUTHORS, INCLUDING:

Kuai Yu
Stanford University
20 PUBLICATIONS **547** CITATIONS
SEE PROFILE

Benxia Li
Anhui University of science and technology
40 PUBLICATIONS **1,396** CITATIONS
SEE PROFILE

THE JOURNAL OF PHYSICAL CHEMISTRY C LETTERS

2008, *112,* 2244−2247
Published on Web 01/25/2008

High-Temperature-Stable Au@SnO_2 Core/Shell Supported Catalyst for CO Oxidation

Kuai Yu, Zhengcui Wu, Qingrui Zhao, Benxia Li, and Yi Xie*

Department of Nanomaterials and Nanochemistry, Hefei National Laboratory for Physical Sciences at Microscale, University of Science and Technology of China, Hefei 230026, P. R. China

Received: December 18, 2007; In Final Form: January 14, 2008

High-temperature-stable Au@SnO_2 core/shell supported catalyst was prepared by a simple intermetallics-based dry-oxidation approach in which the size of the core can be controlled easily by varying the size of the pre-made Au seeds. The change of their structure was investigated by X-ray diffraction (XRD), transmission electron microscopy (TEM), and X-ray photoelectron spectroscopy (XPS). In the as-prepared supported catalysts, Au particles with a mean size of ca. 15 nm were highly encapsulated by the SnO_2 shell. Moreover, the Au@SnO_2 core/shell supported catalysts showed superior catalytic activity compared to non-encapsulated Au−SnO_2. XPS spectra showed that the interactions between the Au catalyst and oxide support in the well-encapsulated Au@SnO_2 core/shell nanoparticles are much stronger than those in the non-encapsulated Au−SnO_2 nanoparticles, further indicating the synergetic confinement effect in such nanoscaled catalyst/support core/shell systems.

Recently, materials with multicomponent functional properties have been the subject of extensive research in contrast with their single-component compounds because the synergistic interactions between each component could strongly affect the properties.[1] Among them, oxide-supported gold nanocomposites had long been regarded for the highly efficient catalysts in many areas, such as CO oxidation, water-gas shift reaction, NO reduction, oxidation of hydrocarbons, and so forth.[2−4] In these applications, CO oxidation over the supported gold nanoparticles has been investigated the most extensively since 1987 when Haruta[5] highlighted the remarkable high activity of supported gold catalysts for low-temperature CO oxidation. However, the gold nanoparticles are unstable against sintering, accompanied by a corresponding loss of catalytic activity, which is a serious problem in many applications. This is caused by the increased mobility of the gold particles on the support at higher temperatures.[6] Therefore, deliberate tailoring of the nanostructured catalysts and optimization of the catalyst structure are still under broad investigation. In addition, the poisoning and deactivating of the Au particles inevitably exist in the conventional solution-based methods, such as coprecipitation[7] and deposition-precipitation,[8,9] in which chloride can adsorb on the gold active sites. Consequently, an ideal catalyst should in general be developed into aggregation- and poison-resistant catalyst of high catalytic activities. One example is to create the core/shell structure.[10] The growth of oxide shell over the gold particles in wet chemical approaches usually needed a pre-covered silica layer modifying the gold surfaces.[6,11] However, it should be noted that the introduction of silica at the interface between the Au particles and the catalyst supports usually leads to a depressed catalytic activity.[12] As a result, preparation of core/shell supported catalysts avoiding the solution-based method and the silica buffer layer are necessary.

* To whom correspondence should be addressed. Tel and Fax: 86-551-3603987. E-mail: yxie@ustc.edu.cn.

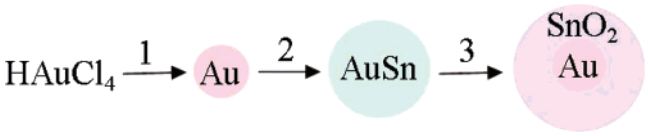

Figure 1. Schematic illustration of the synthesis of Au@SnO_2 core/shell nanoparticles. (Step 1) Au nanoparticles were prepared from the reduction of $HAuCl_4$ solution. (Step 2) AuSn nanoparticles were prepared by the reduction of Sn^{2+} in the presence of pre-made Au nanoparticles at room temperature. (Step 3) The AuSn particles were heated in air by a three-step oxidation process.[17]

In this work, an intermetallics-based dry oxidation method was further developed to produce the metal@oxide core/shell structures, in which an oxide shell was grown directly from one component of the intermetallics by selective oxidation. Very recently, intermetallic compounds were used as the precursors to produce the composite catalysts.[13] However, in this paper, the diverse catalyst structures are realized and they showed a different catalytic performance, which should be influenced by the interfacial interactions between the catalyst and the support. Moreover, giving the large number of intermetallics that are accessible as nanoparticles,[14,15] this method is versatile to yield many other metal@oxide core/shell structures, which could serve as an alternative way for preparing the core/shell supported catalysts. To demonstrate its wide applicability, Au@SnO_2 core/shell nanoparticles were prepared successfully using AuSn as the precursor. Here, SnO_2 was chosen as the shell because of its large number of oxygen vacancies that are believed to promote the CO oxidation reaction.[16]

The pathway leading to the Au@SnO_2 core/shell structure is shown schematically in Figure 1. In brief, the AuSn intermetallic compound was first prepared at room temperature using a freshly prepared solution of dilute $NaBH_4$ to reduce the $SnCl_2$ solution in the presence of pre-made Au nanoparticles as nucleation seeds (Supporting Information, S1). Next, ethanol dispersed AuSn

10.1021/jp711880e CCC: $40.75

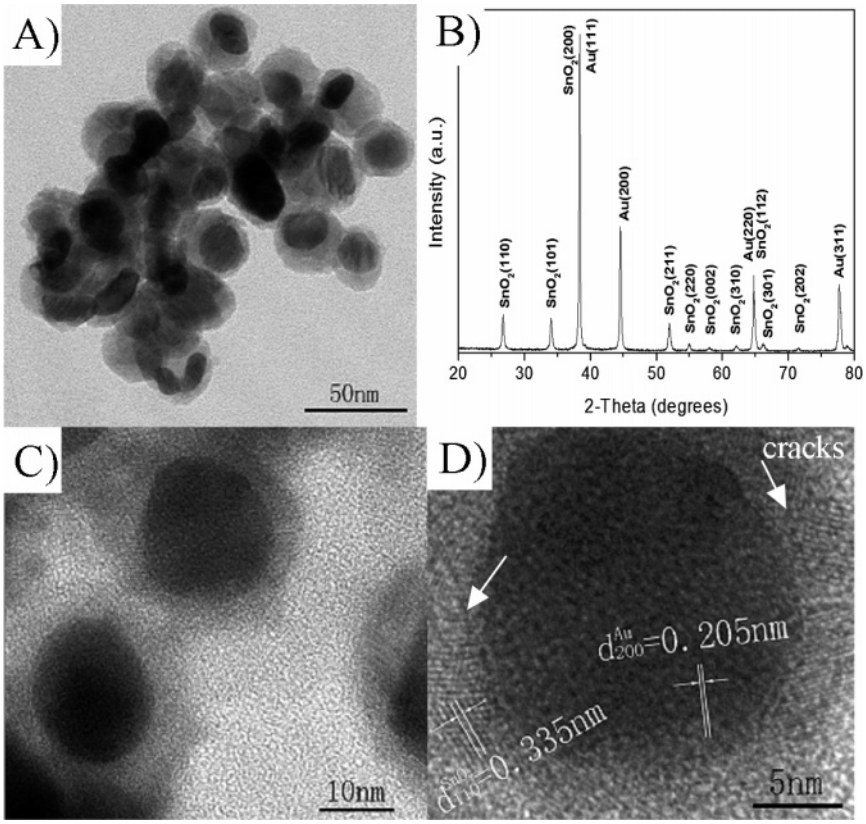

Figure 2. (A) TEM image of the Au@SnO_2 core/shell structure, which clearly shows the Au particles surrounded by a SnO_2 layer. (B) XRD pattern of the as-obtained Au@SnO_2. (C and D) HRTEM images of the core/shell particles, which the lattice distances agree with the (200) plane of Au and (110) plane of SnO_2, respectively. The inset arrows point out the cracks that appeared in a particle.

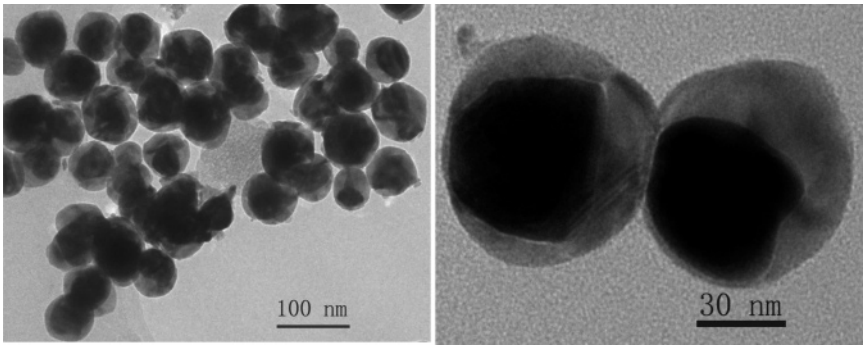

Figure 3. TEM (left) and the corresponding enlarged HRTEM (right) image of Au@SnO_2 core/shell structure with an Au core of 40 nm.

colloids were deposited on a silicon substrate and dried in air. The substrate was then placed inside a furnace to allow the AuSn nanoparticles to be oxidized for a period of time under certain temperatures.

The final products with the core/shell structures were collected on a silicon substrate through a three-step oxidation process (Supporting Information, S2) for all-sided characterization. The X-ray diffraction (XRD) patterns (Figure 2B) showed the two mixed phases of cubic Au (JCPDS card no. 01-1172) and tetragonal SnO_2 (JCPDS card no. 21-1250), which indicated that the AuSn was fully oxidized to the polycrystalline SnO_2 shells enwrapping the Au cores. The contrast between the core and the shell of the nanoparticles was easily distinguishable in the transmission electron microscope (TEM) images as shown in Figure 2. The thickness of the shell was 6−7 nm, and the final size of the Au@SnO_2 nanoparticles was in accordance with the AuSn nanoparticles. As shown in Figure 2C and D, the inner core and the external layer had the lattice spacing values of 0.205 and 0.335 nm that can be indexed to the (200) plane of Au and the (110) plane of SnO_2, respectively. In addition, to testify this tunable method, Au@SnO_2 core/shell structures were also prepared using 40 nm gold particles as seeds shown in Figure 3. It is clear that, after the three-step oxidation process, the particles are finally converted to well-encapsulated Au@SnO_2 core/shell nanoparticles. The last three-step oxidation is analogous to In/In_2O_3[17] based on the Kirkendall effect[18] in which the In_2O_3 shell originated from the oxidation of In, whereas in our approach the heterogeneous metal@oxide core/shell nanostructure originated from the selective oxidation of the intermetallic precursor. In the oxidation process, the tin atoms were oxidized slowly and the content of the soluble tin in gold was decreased. Finally, the tin atoms would be further oxidized to the well-encapsulated Au@SnO_2 core/shell structure. Careful observation can find that some cracks appeared in the SnO_2 shell as shown in Figure 2D. These kinds of cracks in shells of the core/shell particles are due to the different diffusion rates

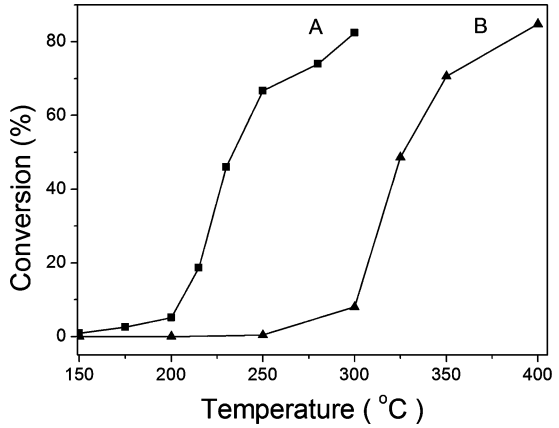

Figure 4. Catalytic performance of the different samples oxidizing at 850 °C for 1 h. The activities of the catalysts for the oxidation of CO were measured in a continuous-flow reactor. The reaction gas, a mixture composition of 10% CO in air (from Air Liquid, 99.99% purity), was fed to a 50 mg catalyst at a rate of 70 mL min^{-1}, which corresponds to a space velocity of 84 000 $cm^3h^{-1}g_{cat}^{-1}$. (A) Well-encapsulated Au@SnO_2 core/shell structure as catalyst. (B) Non-encapsulated Au−SnO_2 structure as catalyst.

of the core material and the shell material.[19] For this particular system, the diffusion of O atoms was faster than that of Sn atoms, leading to the formation of cracks in the shell. From the viewpoint of the catalysts, the cracks may offer more pathways for the small molecules to contact with the catalyst, which may facilitate the catalytic process.[20] Good performance can therefore be expected in heterogeneous catalytic reactions.

One of the standard reactions investigated over gold-supported catalysts is the oxidation of CO. Normally, catalysts are highly active only if the Au particles are smaller than 5 nm. For 15-nm Au particles, only very low activity would be expected.[6] However, for our Au@SnO_2 core/shell catalyst, the temperature for half conversion is about 230 °C, as shown in Figure 4A, which is quite good for this particle size. In particular, the sample had already been heated to 850 °C, implying that the catalyst is high-temperature stable. The high activity of the as-prepared Au@SnO_2 core/shell structure may be related to the synergetic confinement effect, which was named by Bao[21,22] in the case of metal/C nanotubes, in that the metal nanoparticles inside the carbon nanotubes are more active than those loaded outside of the nanotubes. This phenomenon is due to the peculiar interaction of the metal particles with the interior nanotube surface. In our case, the synergetic confinement effect may also exist in this Au@SnO_2 core/shell structure. The Au nanoparticles inside or outside the oxide support could also lead to different synergetic interactions and Au catalytic activity. To check whether the encapsulation of SnO_2 on Au particles is favorable for the catalytic activity, we prepared a reference sample with non-encapsulated Au−SnO_2 catalyst by a fast oxidation process (Supporting Information, S3) and tested it as a catalyst for the CO oxidation. For the non-encapsulated Au−SnO_2 catalyst, the temperature for half conversion is about 330 °C, as shown in Figure 4B, 100 °C higher than that for the Au@SnO_2 core/shell catalyst. Notably, the non-encapsulated Au−SnO_2 catalyst suffers a substantial loss in activity compared to the well-encapsulated Au@SnO_2.

To give more evidence for this synergetic confinement effect in the Au@SnO_2 core/shell structure as a catalyst, we employed X-ray photoelectron spectroscopy (XPS) to study the interactions between the metal catalyst and oxide support. Important information about the electronic structure of the catalyst can be provided by XPS, as shown in Figure 5A. The lowest Au4$f_{7/2}$

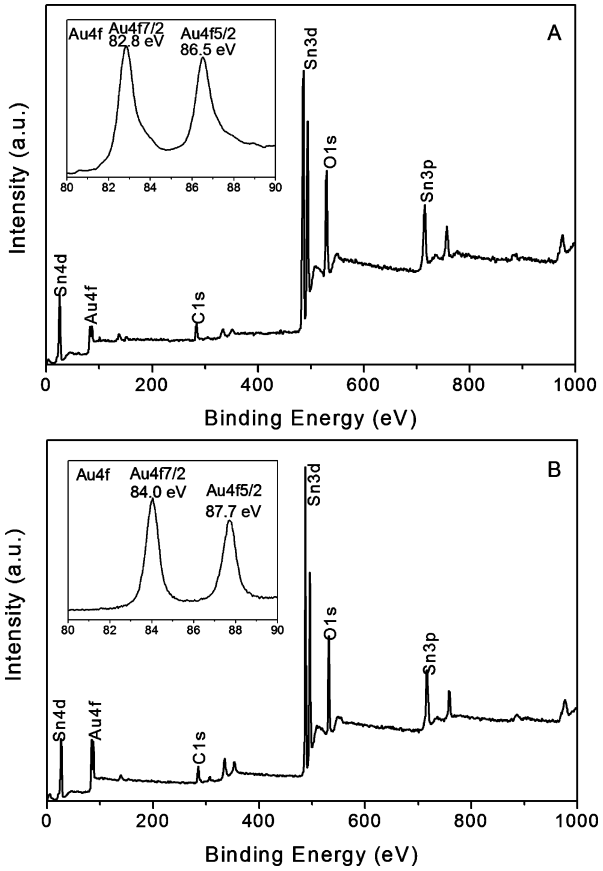

Figure 5. XPS spectra of (A) the well-encapsulated Au@SnO_2 core/shell nanoparticles and (B) the non-encapsulated Au−SnO_2 nanoparticles. The inset is the corresponding Au 4f region.

electron binding energy (BE) level was located at 82.8 eV for the well-encapsulated Au@SnO_2. No peaks corresponding to oxidized species, located around 85.5 and 86.3 eV, have been detected,[14] implying that Au in the Au@SnO_2 core/shell structure is in a metallic state. Interestingly, the Au 4$f_{7/2}$ spectrum in Figure 5A shows a negative BE shift of −1.3 eV with respect to that of bulk metallic Au (84.1 eV). It is known that the Au 4$f_{7/2}$ electrons with a BE lower than that of bulk atoms for the Au-support nanocomposites might be ascribed to two factors:[23] the small size of the Au clusters (<1 nm) and electronic structure differences between the support and the Au nanoparticles. In the present study, the gold particles are much larger than 1 nm; thus, the first possibility was discarded. Meanwhile, the electron transfer from the oxide support to the Au particles should be the major contribution to the observed shift. Therefore, the strong interactions between Au and oxide support exist in this encapsulated Au@SnO_2 core/shell structure, which may enhance its catalytic performance for CO oxidation. It is expected that the Au@SnO_2 core/shell structure had larger interaction areas than the non-encapsulated Au−SnO_2 structure, leading to the stronger metal−support interactions. For comparison, XPS spectra of the non-encapsulated Au−SnO_2 was also collected, as shown in the Figure 5B, in which the lowest Au4$f_{7/2}$ BE level was located at 84.0 eV, with almost no BE shift compared to the bulk metallic Au. XPS results clearly indicate that much stronger interactions exist between the Au particles and the support in the well-encapsulated Au@SnO_2 than in the non-encapsulated Au−SnO_2, confirming that the strong interactions in the Au@SnO_2 core/shell structure lead to the high catalytic performance. In addition, the poison-free gold

surfaces may also enhance the catalytic performance. However, further studies are needed about the details of the catalytic mechanism.

In summary, $Au@SnO_2$ core/shell nanocomposites were first prepared by a simple intermetallics-based dry-oxidation approach in which the size of the core and the shell can be controlled easily by varying the initial conditions of the reactants. Because of the synergetic confinement effect of $Au@SnO_2$, the well-encapsulated core/shell nanoparticles show efficient and high-temperature-stable CO catalytic activity. XPS spectra show that the interactions between the Au catalyst and oxide support in the well-encapsulated $Au@SnO_2$ core/shell nanoparticles are much stronger than those in the non-encapsulated $Au-SnO_2$ nanoparticles, which provides direct and cogent support in the synergetic confinement effect in the nanoscaled catalyst@support core/shell system. Moreover, $Au@SnO_2$ core/shell nanocomposites may also find applications in electrocatalysis and gas sensors. This simple dry-oxidation approach to the $Au@SnO_2$ core/shell catalyst is easily to scale up, which may be potentially applied in the areas of technology and industry and also has the potential to yield many other metal@oxide core/shell supported catalysts using the binary or ternary intermetallics as the precursors.

Acknowledgment. This work was financially supported by the National Natural Science Foundation of China (no. 20621061).

Supporting Information Available: Detailed experimental sections and the characterization of the AuSn intermetallic compound. This material is available free of charge via the Internet at http://pubs.acs.org.

References and Notes

(1) Li, J. B.; Wang, L. W. *Appl. Phys. Lett.* **2004**, 3649.

(2) Xu, C.; Su, J.; Xu, X.; Liu, P.; Zhao, H.; Tian, F.; Ding, Y. *J. Am. Chem. Soc.* **2007**, *129*, 42.

(3) Lomello-Tafin, M.; Chaou, A. A.; Morfin, F.; Caps, V.; Rousset, J. *Chem. Commum.* **2005**, 388.

(4) Mohapatra, P.; Moma, J.; Parida, K. M.; Jordaan, W. A.; Scurrell, M. S. *Chem. Commum.* **2007**, 1044.

(5) Haruta, M.; Kobayashi, T.; Sano, H.; Yamada, N. *Chem. Lett.* **1987**, 405.

(6) Arnal, P. M.; Comotti, M.; Schüth, F. *Angew. Chem., Int. Ed.* **2006**, *45*, 8224.

(7) Sanchez, R. M. T.; Ueda, A.; Tanaka, K.; Haruta, M. *J. Catal.* **1997**, *168*, 125.

(8) Zheng, N.; Stucky, G. D. *J. Am. Chem. Soc.* **2006**, *128*, 14278.

(9) Zhong, Z.; Lin, J.; Teh, S.; Teo, J.; Dautzenberg, F. M. *Adv. Funct. Mater.* **2007**, *17*, 1402.

(10) Zhong, C.; Maye, M. M. *Adv. Mater.* **2001**, *13*, 1507.

(11) Lou, X. W.; Yuan, C.; Archer, L. A. *Small* **2007**, *3*, 261.

(12) Chiang, C. W.; Wang, A.; Wan, B. Z.; Mou, C. Y. *J. Phys. Chem. B* **2005**, *109*, 18042.

(13) (a) Dawood, F.; Leonard, B. M.; Schaak, R. E. *Chem. Mater.* **2007**, *19*, 4545. (b) Kamiuchi, N.; Matsui, T.; Kikuchi, R.; Eguchi, K. *J. Phys. Chem. C* **2007**, *111*, 16470.

(14) (a) Sra, A. K.; Ewers, T. D.; Schaak, R. E. *Chem. Mater.* **2005**, *17*, 758. (b) Cable, R. E.; Schaak, R. E. *Chem. Mater.* **2005**, *17*, 6835.

(15) (a) Leonard, B. M.; Bhuvanesh, N. S. P.; Schaak, R. E. *J. Am. Chem. Soc.* **2005**, *127*, 7326. (b) Leonard, B. M.; Schaak, R. E. *J. Am. Chem. Soc.* **2006**, *128*, 11475.

(16) Meyer, R.; Lemire, C.; Shaikhutdinov, S. K.; Freund, H. J. *Gold Bull.* **2004**, *37/1−2*, 72.

(17) Lei, Y.; Chim, W. *J. Am. Chem. Soc*. **2005**, *127*, 1487.

(18) Yin, Y.; Rious, R. M.; Erdonmez, C. K.; Hughes, S.; Somorjai, G. A.; Alivisatos, A. P. *Science* **2004**, *304*, 711.

(19) Wang, Y.; Cai, L.; Xia, Y. *Adv. Mater.* **2005**, *17*, 473.

(20) Kim, S.; Yin, Y.; Alivisatos, A. P.; Somorjai, G. A.; Yates, J. T. *J. Am. Chem. Soc.* **2007**, *129*, 9510.

(21) Pan, X.; Fan, Z.; Chen, W.; Ding, Y.; Luo, H.; Bao, X. *Nat. Mater*. **2007**, *6*, 507.

(22) Chen, W.; Pan, X.; Bao, X. *J. Am. Chem. Soc.* **2007**, *129*, 7421.

(23) Tian, C.; Mao, B.; Wang, E.; Kang, Z.; Song, Y.; Wang, C.; Li, S. *J. Phys. Chem. C* **2007**, *111*, 3651.